Eur. Phys. J. D **34**, 173–176 (2005)
DOI: 10.1140/epjd/e2005-00134-5

THE EUROPEAN PHYSICAL JOURNAL D

# Formation and characterization of high-density Fe cluster-assembled films with soft magnetic behaviors

D.L. Peng[1,a], H. Yamada[1], K. Sumiyama[1], T. Uchida[2], and T. Hihara[1]

[1] Department of Materials Science and Engineering, Nagoya Institute of Technology, 466-8555 Nagoya, Japan
[2] Department of Applied Chemistry, Nagoya Institute of Technology, 466-8555 Nagoya, Japan

Received 6 September 2004
Published online 13 July 2005 – 

**Abstract.** High-density, magnetically soft Fe cluster-assembled films were obtained at room temperature by an energetic cluster deposition. Size-monodispersed Fe clusters with the mean cluster size $d = 9$, 13 and 16 nm were produced using a plasma-gas-condensation technique. Ionized clusters in cluster beam were accelerated electrically and deposited onto the substrate together with neutral clusters from the same cluster source. The morphology, microstructure and magnetic properties of the cluster-assembled films have been studied by an atomic force microscopy, scanning electron microscopy, transmission electron microscopy, and superconducting quantum interference device magnetometer. By increasing the impact energy of the ionized clusters up to 0.6 eV/atom, the Fe cluster-assembled film has a packing fraction of $0.86 \pm 0.03$, and reveals a soft magnetic behavior. In addition, it is found that oxidization of the cluster-assembled films is remarkably suppressed with the increase in the density of the films.

**PACS.** 81.07.-b Nanoscale materials and structures: fabrication and characterization – 61.46.+w Nanoscale materials: clusters, nanoparticles, nanotubes, and nanocrystals – 75.75.+a Magnetic properties of nanostructures

## 1 Introduction

Cluster-assembling method is a promising alternative to fabricate nanoscale structure-controlled materials. However, cluster-assembled films formed by cluster soft-landing, in which the initial cluster size is maintained, have a porous structure. Such a low density (about 30% of the bulk) leads to a large coercivity value and a low magnetic flux density. Therefore, it is interesting to find a way to increase the density of the cluster-assembled films and then obtain the soft magnetic properties. Generally, the soft magnetic properties of nanocrystalline films originate from the fine grain size and strong intergrain ferromagnetic exchange coupling between the grains. When the grains are in contact, a magnetic exchange interaction across the interfaces is then possible. When the grain size of such materials is comparable to the effective bulk domain-wall width, the magnetization may not follow the randomly oriented easy axis of each individual grain, and a common alignment of the magnetization in correlated grains may occur. The magnetocrystalline anisotropy constant may then be averaged over several grains (namely, the magnetocrystalline anisotropy is reduced) with the consequence that the coercivity decreases with decreasing grain size. This model is known as the random anisotropy model (RAM) [1].

The use of clusters to generate bulk nanocrystalline materials and thin films has been explored by several groups [2–7]. Gleiter et al. have first reported nanocrystalline materials by collection and consolidation of small metallic clusters [2,3]. Using a gas-deposition method, Sasaki et al. have also produced high-density nanocrystalline films [4,5]. In this method, a large pressure difference between an evaporation chamber and a deposition chamber was utilized. Based on an energetic cluster impact (ECI) concept, Haberland et al. [6,7] clearly demonstrated the effect of accelerating energy of incident clusters on thin film deposition and its morphology using an alternative sputtering-type cluster source. In this technique, electrically charged clusters are accelerated by an electric field of an order of kV and directed onto the substrate.

For the deposition of free clusters on substrates, a crucial parameter is the energy per atom in the free cluster. Roughly, we distinguish three regimes depending on the impact energy value [8,9]. (1) The low energy regime corresponds to the case of free clusters with an impact energy of about or lower than 0.1 eV per atom. In this case, one could expect the memory of the free clusters without fragmentation and structural rearrangement during the film growth on the substrate, and the resulting films are black and porous. (2) At a medium energy regime of

[a] e-mail: pengdl@ss.mse.nitech.ac.jp

about 1 eV per atom, the films are colored with a better adhesion. (3) In the high energy regime (about or larger than 10 eV per atom), the fragmentation of the clusters occurs and strongly adhering, mirrorlike films appear.

In this paper, we demonstrate a simple preparation method of magnetically soft Fe cluster-assembled films by ECI deposition at room temperature. We will show that mixing deposition of electrically accelerated, charged Fe clusters and neutral ones from the same cluster source can produce a high-density Fe cluster-assembled films which reveal a good soft magnetic property.

## 2 Experimental

The samples were prepared by a plasma-gas-condensation (PGC)-type cluster beam deposition apparatus [10,11], which is based on plasma-glow-discharge vaporization (sputtering) and inert gas condensation techniques. The background pressure of all chambers (sputtering, cluster-forming and depositing chambers) was $<1.3 \times 10^{-5}$ Pa. During cluster deposition, a large amount of 99.9999% purity Ar and 99.99995% purity He gases of $1.87-4.1 \times 10^{-4}$ mol/s were introduced continuously into the sputtering chamber and evacuated by a mechanical booster pump through a nozzle, making the sputtering chamber pressure approximately $1-7 \times 10^2$ Pa. Fe atoms sputtered into the inert gas space are decelerated by collisions with Ar and He gas atoms and collide with each other to form Fe clusters. Fe clusters are partially charged and no additional ionization process is necessary for ionizing clusters because they reside in the plasma region where the electron and ion densities are high [6,7]. Based upon deposition experiments of total and charged Fe clusters, we roughly estimated that there are about 20% positively charged clusters, 20% negatively charged clusters and 60% neutral clusters in our Fe cluster beam. The large clusters, which are formed in the cluster growth room and cooled by liquid nitrogen, are ejected from a small nozzle by differential pumping and a part of the cluster beam is intercepted by two skimmers, and then deposited onto a metallic sample holder which can be kept at a voltage $V_a$ up to $\pm 25$ kV in the deposition chamber ($7-10 \times 10^{-3}$ Pa). In this experiment, we applied negative $V_a$ from 0 to $-20$ kV, and obtained the Fe cluster-assembled films consisting of neutral clusters and positive charged clusters which are accelerated by $V_a$. We deposited Fe clusters on transmission electron microscopy (TEM) microgrids for TEM observation and on Si wafers for scanning electron microscopy (SEM) and atomic force microscopy (AFM) observation, and magnetic measurement. Magnetization was observed using a superconducting quantum interference device magnetometer.

## 3 Results and discussion

Figures 1a, 1b and 1c show typical bright-field (BF) TEM images of the initial Fe clusters with effective thickness

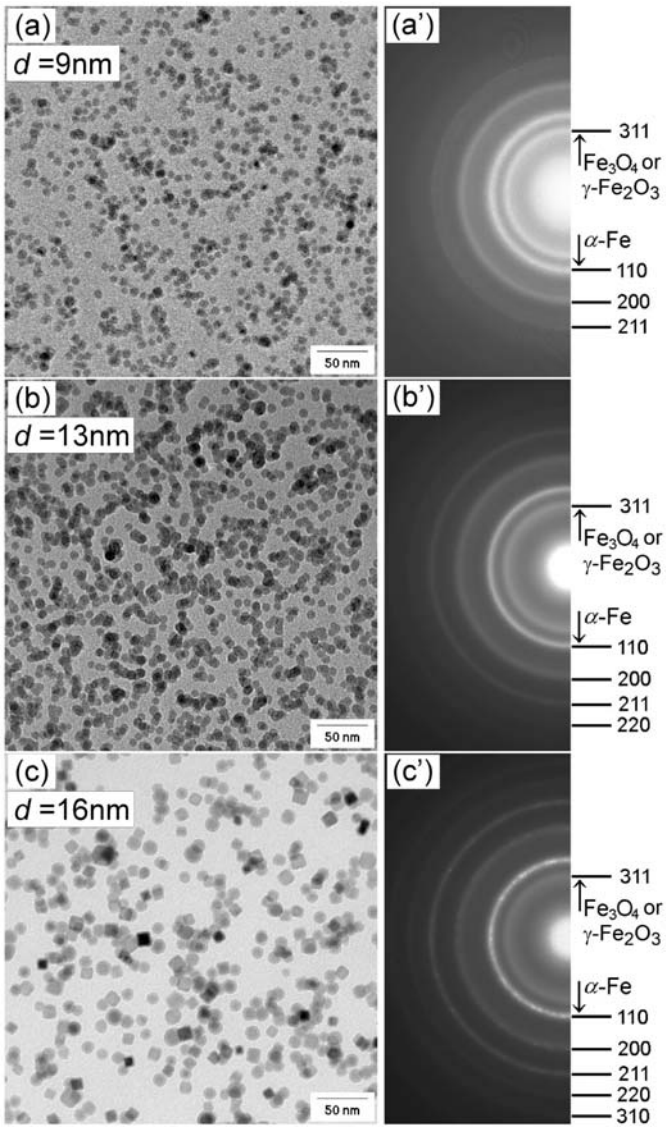


**Fig. 1.** HRTEM BF images (a, b, and c) of images and ED patterns (a', b', and c') of the initial Fe clusters deposited at $V_a = 0$ kV and under different Ar and He gas flow rates: (a, a') $R_{Ar} = 1.86 \times 10^{-4}$ and $R_{He} = 4.1 \times 10^{-4}$ mol/s, (b, b') $1.86 \times 10^{-4}$ and $2.61 \times 10^{-4}$ mol/s, and (c, c') $2.24 \times 10^{-4}$ and 0 mol/s, respectively.

$t_e \approx 2.5$ nm prepared at $V_a = 0$ kV and under different Ar and He gas flow rates: (a) $R_{Ar} = 1.86 \times 10^{-4}$ and $R_{He} = 4.1 \times 10^{-4}$ mol/s, (b) $1.86 \times 10^{-4}$ and $2.61 \times 10^{-4}$ mol/s, and (c) $2.24 \times 10^{-4}$ and 0 mol/s, respectively. From TEM images, spherical or cubic shape Fe clusters can be seen and their size is almost monodispersive. The mean cluster diameter, $d$, increases from 9 to 16 nm with decreasing $R_{He}$ from $4.1 \times 10^{-4}$ to 0 mol/s. The electron diffraction (ED) patterns of corresponding heavily stacked cluster assemblies are shown in Figures 1a', 1b', and 1c'. The ED patterns of these Fe clusters all mainly display one set of diffraction rings of a body-centered-cubic (bcc) $\alpha$-Fe structure for $d = 9$, 13, and 16 nm. There is a ring corresponding to {311} of $Fe_3O_4$

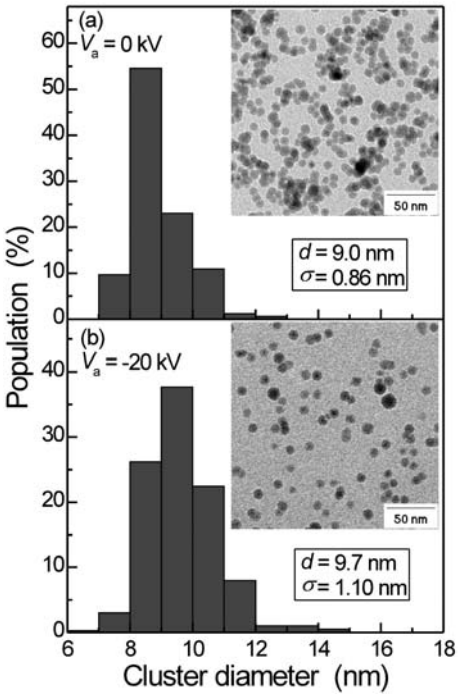


**Fig. 2.** Size distribution of the Fe clusters deposited at (a) $V_a = 0$ and (b) $-20$ kV. The insets show the BF TEM images of Fe cluster-assembled films at the initial deposition stages for $V_a = 0$ and $-20$ kV.

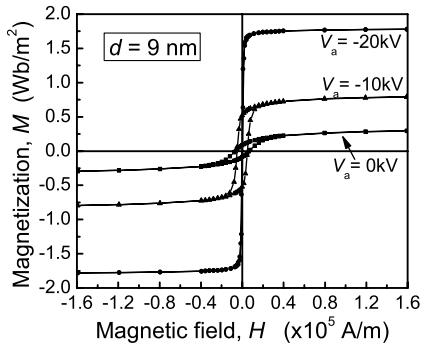


**Fig. 3.** In-plane hysteresis loops of the Fe cluster-assembled films deposited by ECI with different acceleration voltages. The initial mean cluster size was $d = 9$ nm.

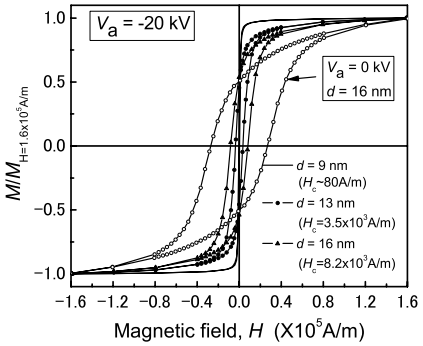


**Fig. 4.** In-plane hysteresis loops of the Fe cluster-assembled films deposited by ECI with different initial mean cluster sizes. The acceleration voltage was retained at $V_a = -20$ kV. The open-circle-line shows the loop of the Fe clusters with the same initial cluster size $d = 16$ nm deposited at $V_a = 0$ kV.

or $\gamma$-$Fe_2O_3$ phase, where it is not possible to differentiate between these two phases by ED because their lattice parameters are very similar. This is due to partial oxidation of the cluster assembly only by exposing it to the ambient atmosphere.

In order to examine the difference between cluster sizes under $V_a = 0$ and $-20$ kV, we carried out TEM observations for Fe cluster-assembled films with effective thicknesses of about 2.5 (upper) and 1.5 nm (lower) (see the insets in Fig. 2). Figure 2 shows the cluster size distributions which were measured precisely for about 400 clusters using an image-analysis software (Image-Pro PLUS: Media Cybernetics) for the digitized images recorded by a slow scan CCD camera. The estimated mean cluster sizes is $d = 9.0$ and 9.7 nm with standard deviations $\sigma = 0.86$ and 1.1 nm for $V_a = 0$ and $-20$ kV, respectively. Both $d$ and $\sigma$ values for $V_a = -20$ kV are slightly larger than that for $V_a = 0$ kV. According to the measurement results of translational velocity of Ag clusters in supersonic adiabatic expansion through a small nozzle into vacuum [12], we estimated the impact energy of Fe clusters under $V_a = 0$ kV to be about 0.07 eV/atom using a translational velocity of 500 m/s, belonging in the low energy regime. For $V_a = -20$ kV, the impact energy of clusters under $V_a = -20$ kV is estimated to be about 0.6 eV/atom for $d = 9$ nm. This energy value is one order larger than that of Fe clusters before acceleration (namely, $V_a = 0$ kV), but it is one order lower than the cohesive energy of Fe (4.47 eV/atom). Therefore, it is suggested that in the present cluster-assembled films by ECI a part of Fe clusters were deformed and/or destroyed while the size of most of Fe clusters was not increased remarkably.

Figure 3 shows the in-plane hysteresis loops of the Fe cluster-assembled films deposited on room temperature substrates by ECI with different $V_a$ values, where $d = 9$ nm. The magnetization is saturated more rapidly and a soft magnetic behavior was observed with increasing $V_a$. From the random anisotropy model for nanocrystalline materials [1], the soft magnetic property strongly depends on the grain size. Here, we also show the size dependence of in-plane hysteresis loop for the Fe cluster-assembled films deposited by ECI with $V_a = -20$ kV in Figure 4. With increasing the cluster size, coercivity, $H_c$, rapidly increases and the magnetization is saturated more slowly. To further compare the magnetic behavior between the samples with the initial mean cluster size of $d = 16$ nm, the in-plane hysteresis loops of the Fe cluster-assembled films deposited under $V_a = 0$ kV is also given in Figure 4 (shown by a open-circle-line). Clearly, $H_c$ was also decreased remarkably with increasing $V_a$ although its value is not so low as that for $d = 9$ nm. These results indicate that in order to obtain the soft magnetic property it is important to use the initial clusters with a suitable size.

Figure 5 shows the packing fraction, $P$, and $H_c$ as a function of $V_a$. As seen from this figure, $P$ increases rapidly with increasing $V_a$. For $V_a = 0$ kV, $P$ is only 0.31 while

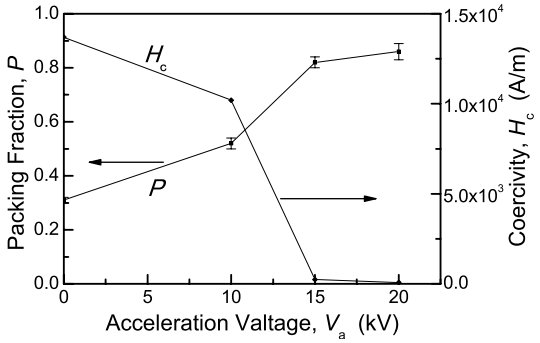


**Fig. 5.** The $V_a$ dependence of the packing fraction, $P$, and coercivity, $H_c$, of the Fe cluster-assembled films deposited by ECI. The initial mean cluster size was $d = 9$ nm.

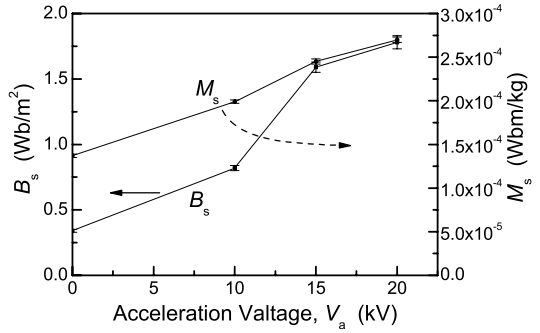


**Fig. 6.** The $V_a$ dependence of the saturation magnetic flux density, $B_s$, and saturation magnetization per weight, $M_s$, of the Fe cluster-assembled films deposited by ECI. The initial mean cluster size was $d = 9$ nm.

$P$ increases up to 0.86 when $V_a = -20$ kV. $H_c$ dramatically decreases with increasing $V_a$. For $V_a = -20$ kV, $H_c$ becomes smaller than 80 A/m. This $H_c$ value is lower than that ($H_c > 200$ A/m) for pure Fe thin films [13,14]. It is thought that the lower coercivity is realized by the higher $V_a$ which leads to the increase of $P$ in the cluster-assembled films.

Figure 6 shows saturation magnetic flux density, $B_s$, and saturation magnetization per weight, $M_s$, as a function of $V_a$. Clearly, $B_s$ increases rapidly with increasing $V_a$ due to the increase of $P$. For $V_a = -20$ kV, $B_s$ reaches up to 1.78 Wb/m$^2$ (namely about 83% of $B_s$ of bulk $\alpha$-iron). On the other hand, $M_s$ also rapidly increases with increasing $V_a$ (namely $P$). This shows that the degree of oxidization is also remarkably reduced with increasing $P$. For $V_a = 0$ kV, $M_s$ is only $1.37 \times 10^{-4}$ Wbm/kg (about 50% of that of bulk Fe ($2.75 \times 10^{-4}$ Wbm/kg)) while $M_s$ increases up to $2.70 \times 10^{-4}$ Wbm/kg (about 98% of that of bulk Fe) when $V_a = -20$ kV, which is suggested that the surfaces of the clusters are hardly exposed to the air since each of clusters is packed closely.

## 4 Conclusion

We have employed plasma-gas-condensation technique and energetic cluster impact method to produce high-density Fe cluster-assembled films with soft magnetic properties. The accelerating voltage and initial cluster size play important roles on increasing the density of the Fe cluster-assembled films and realizing the soft magnetic behavior. For given cluster size, packing fraction and saturation magnetic flux density increase rapidly and magnetic coercivity decreases rapidly with increasing the acceleration voltage. In particular, the oxidization of the cluster-assembled films is remarkably suppressed with the increase in the density of the films.

These works have been supported by Intellectual Cluster Project of the Ministry of Education, Science, Culture and Sports, Japan, Aichi Prefecture, Nagoya City and Aichi Science and Technology Foundation, by a Grant-in-Aid for Scientific Research of the Ministry of Education, Science, Culture and Sports, Japan, and by NITECH 21st Century COE Program "World Ceramics Center for Environmental Harmony". We appreciate Mr. K. Takada for his experimental assistance in the atomic absorption spectroscopy measurement.

## References

1. G. Herzer, IEEE Trans. Magn. **26**, 1397 (1990)
2. H. Gleiter, Progr. Mat. Sci. **33**, 223 (1988)
3. R. Birringer, U. Herr, H. Gleiter, Suppl. Trans. Jpn Inst. Matels **27**, 43 (1986)
4. Y. Sasaki, K. Shiozawa, H. Tanimoto, Y. Iwamoto, E. Kita, A. Tasaki, Mater. Sci. Eng. A **217/218**, 344 (1996)
5. Y. Sasaki, M. Hyakkai, E. Kita, A. Tasaki, H. Tanimoto, Y. Iwamoto, J. Appl. Phys. **81**, 4736 (1997)
6. H. Haberland, M. Karrais, M. Mall, Y. Thurner, J. Vac. Sci. Technol. A **10**, 3266 (1992)
7. H. Haberland, M. Mall, M. Moseler, Y. Qiang, T. Reiners, Y. Thurner, J. Vac. Sci. Technol. A **12**, 2925 (1994)
8. H. Haberland, Z. Insepov, M. Moseler, Phys. Rev. B **51**, 11061 (1995)
9. P. Melinon, V. Paillard, V. Dupuis, A. Perez, P. Jensen, A. Hoareau, J.P. Perez, J. Tuaillon, M. Broyer, J.L. Vialle, M. Pellarin, B. Baguenard, J. Lerme, Int. J. Mod. Phys. B **9**, 339 (1995)
10. S. Yamamuro, K. Sumiyama, K. Suzuki, J. Appl. Phys. **85**, 483 (1999)
11. D.L. Peng, H. Yamada, T. Hihara, T. Uchida, K. Sumiyama, Appl. Phys. Lett. **85**, 2935 (2004)
12. I. Yamada, G.H. Takaoka, Jpn J. Appl. Phys. **32**, 2121 (1993)
13. S. Iwatsubo, T. Takahashi, M. Naoe, Thin Solid Films **281-282**, 484 (1996)
14. S. Iwatsubo, M. Naoe, J. Appl. Phys. **93**, 7193 (2003)